Audio Engineering Society
Convention Paper 6580

Presented at the 119th Convention
2005 October 7–10 New York, New York USA

Modelling Compression Drivers using T Matrices and Finite Element Analysis

David J Murphy[1], Rick Morgans[2]

[1] Krix Loudspeakers, 14 Chapman Road HACKHAM AU5163 South Australia
dmurphy@krix.com.au

[2] Consultant Krix Loudspeakers, currently PostDoctoral Fellow, CSIRO CMIT
rmorgans@gmail.com

ABSTRACT

Models for a commercial compression driver were developed using transmission line matrices and Finite Element Analysis using the commercial package ANSYS. The models were compared with measurements using plane wave tube loading, and discrepancies investigated. The electrical impedance was measured *in-vacuo* to obtain Thiele-Small parameters without acoustic loading. A resonance was investigated and found to be air leakage into the magnet cavity. The development of frequency dependent damping in the matrix and FEA models was necessary to improve the simulation accuracy.

1. INTRODUCTION

Compression drivers are special moving coil loudspeakers, and when coupled to horns are used as components in high performance audio systems. Figure 1 shows a schematic of such a compression driver. The device converts an electrical input signal into mechanical motion of a diaphragm through an electro-mechanical drive (voice coil and magnet). The movement of the diaphragm produces fluctuations in pressure in front of an abrupt change in area. These pressure fluctuations pass through a series of small channels (a phase plug) to enter the horn at the throat of the flare.

The diaphragm has a much greater mechanical impedance than that of air, and the horn, with a gradual change in cross sectional area from the throat to its mouth, can be considered an acoustic "transformer" of impedance providing a better match and hence better transfer of power. A technique for improving the overall performance, especially in the extension of high frequency response, is to restrict the area of the throat to be significantly less than that of the diaphragm – commonly called a "compression ratio".

Most manufacturers of horn loaded loudspeakers purchase compression drivers from suppliers as pre-fabricated components and generally have little influence over their design. However the compression driver and acoustic horn is a tightly coupled electro-acoustic system, and accurate system models are required for the design of high performance audio equipment [1]. Previous work has been described in the literature using a lumped parameter approach [2] and Finite Element Analysis [3]. This paper uses similar

approaches to model a commercial compression driver, compares both models to experiment, and describes methods used to obtain accurate simulations.

The format of this paper is as follows. The compression driver used in this study is described, the basic theory behind the modelling techniques is outlined, and some details of the T matrix implementation using a mathematical analysis software package are given. The FEA methodology is summarised, comparison results are presented, and conclusions drawn.

A simple cross section diagram of a compression driver [4] is shown in Figure 1

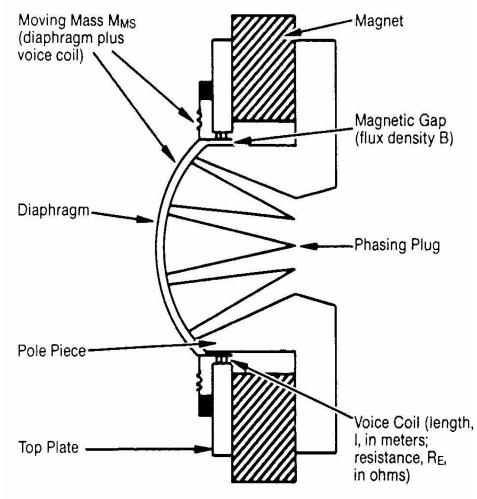

Figure 1 Simplified cross section diagram of a compression driver.

2. COMPRESSION DRIVER GEOMETRY

The compression driver used in this study is a Beyma Model CP800/Ti [5]. It has a titanium diaphragm of 100mm diameter, a 50mm diameter exit throat, a mass of 10.3 kilograms, 60 Watts thermal power dissipation, and a nominal impedance of 8 Ohms. A compression driver was cut in half to investigate its physical layout and verify the manufacturer's engineering drawing. Figure 2 shows a schematic cross section of the device, with an enlarged view of the geometry around the voice coil.

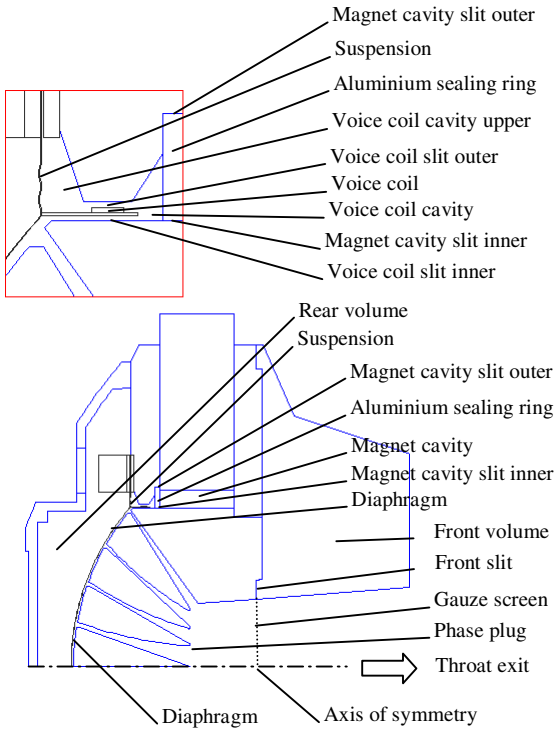

Figure 2 Details of half section of compression driver.

3. MODELLING THEORY

This section describes the theory used in modelling the compression driver, using a relatively simple transmission matrix approach and a more complex numerical method, Finite Element Analysis (FEA)

3.1. Acoustic Equivalent Circuits

A classic paper by Bauer [6] outlines a systematic method for developing the electrical equivalent circuit from an acoustic structure. He developed two systems of analogies, Voltage-Force-Pressure (EFP), and Current-Velocity-Fluid Velocity (IFP). Conversion between them is possible, but some acoustic systems fall more naturally into one or the other. The result of applying his process is an electrical equivalent circuit diagram of the acoustic system.

The EFP and IFP analogy systems are summarized in Table 1. The basic mechanical and acoustic network components are outlined in Figures 3 and 4.

Geometric similarity between an acoustic system and its equivalent electrical circuit comes about naturally using the EFP analogy, especially as a volume can be represented by a grounded capacitor. The physical structures of pipes, capillaries and such, connecting these volumes directly correspond to the electrical components. Developing the equivalent circuits of mechanical structures e.g. moving masses and/or diaphragms, is facilitated by providing configurations of the electrical circuit elements with terminals chosen to have correspondence to the terminals in the respective mechanical circuit elements. A further solution, especially for electro-acoustic transducers, is the use of a gyrator, a four terminal 'black box' the current and voltage of one set being related to the voltage and current of the other set, respectively, by a real constant.

3.2. Transmission Matrix Theory

The transmission matrix method, as outlined in a review paper by Lampton [7], is a versatile method for the analysis of electro-mechanical-acoustic devices. It provides a systematic method for finding the end to end linear transfer characteristic of cascaded electrical networks in terms of the characteristics of the component elements. Lampton also developed a methodology for parallel paths, giving his method more versatility.

The formalism may be extended to include transducers, mechanical components, acoustical devices, and so on, by appropriately generalizing the column vectors so that they describe the variables at each stage of the system, and then defining each T-matrix in such a way as to correctly relate the required column variables. The scheme can be made self consistent providing that at each point the product of the two variables gives the rightward-directed power, in analogy with the electrical case. Furthermore, manipulation of expressions containing these various vectors is considerably simplified if they are kept in a unified impedance form in which the upper component is the scalar drop variable, and the lower is the vector flow variable. With this rationale, the appropriate electrical variables are voltage and rightward flowing current, the mechanical variables are compressive force and rightward directed velocity, and the acoustical variables are pressure and rightward-directed volume velocity. With these choices, shown in (1)

Table 1 Relationships which are the basis of the EFP and IFP analogies

		Electrical Analogy	
Acoustical Quantity	Mechanical Quantity	EFP Analogy	IFP Analogy
Sound Pressure (p)	Force (F)	Voltage (E)	Current (I)
uBar	Dyne		
N/m^2	newton	volt	ampere
Volume velocity (U)	Velocity (v)	Current (I)	Voltage (E)
Volume Displacement (V)	Displacement (D)	Charge (Q)	Impulse
cm^3	cm		
m^3	meter	coulomb	volt-sec
Acoustical Resistance (R_A)	Mechanical Resistance (R_M)	Resistance (R)	Conductance (G)
rayl ($dyn.s/cm^5$)	mech. ohm (dyn.sec/cm)		
MKS-rayl ($N.s/m^5$)	MKS-mech. ohm(N.s/m)	Ohm	Ohm
Inertance (M_A)	Mass (M)	Inductance (L)	Capacitance (C)
g/cm^4	Gram		
kg/m^4	kg	Henry	Farad
Acoustical Compliance (C_A)	Mechanical Compliance (C_M)	Capacitance (C)	Inductance (L)
cm^5/dyn	cm.dyn		
m^5/N	m/N	Farad	Henry
Acoustical Impedance (Z_A)	Mechanical Impedance (Z_M)	Impedance (Z)	Admittance (Y)
$ZA = p/U$	$ZM = F/v$	$Z = E/I$	$Y = I/E$

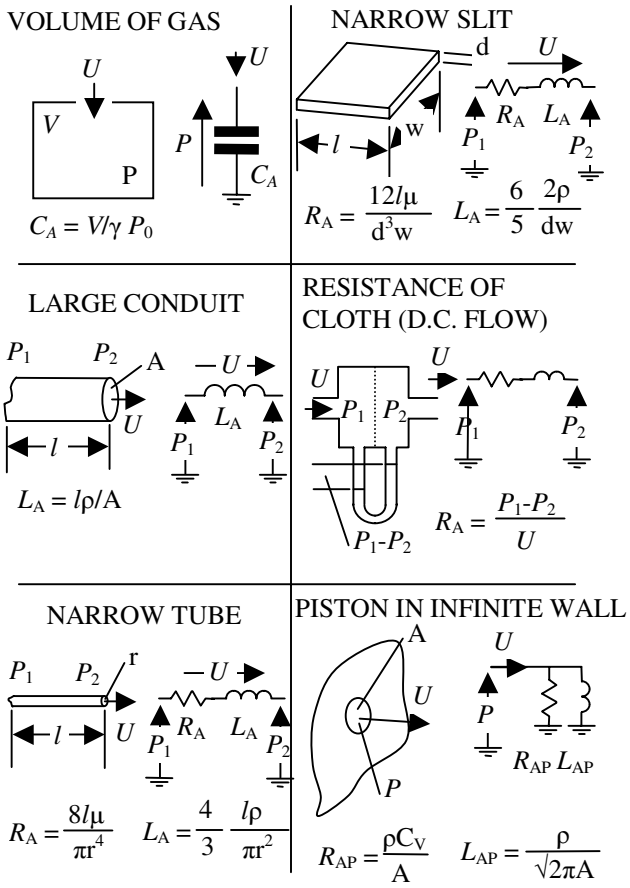

Figure 3 Acoustic Impedance values of the most common elements by EFP analogy

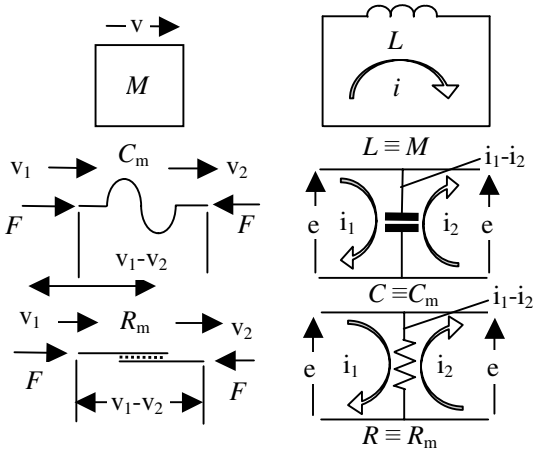

Figure 4 Basic mechanical network elements and equivalent electrical circuits by EFP analogy.

$$\begin{pmatrix} e \\ i \end{pmatrix} \quad or \quad \begin{pmatrix} f \\ v \end{pmatrix} \quad or \quad \begin{pmatrix} p \\ u \end{pmatrix} \tag{1}$$

the effect of the network element which supplies additional impedance is always described by a T-matrix for a series impedance, just as in the electrical case. Similarly, the effect of a circuit element that admits additional flow is described by the basic admittance T-matrix. Elements for a mechanical circuit may be assembled into a T-matrix by writing the mechanical mesh equations in the form shown in equation (2).

$$\begin{pmatrix} f_1 \\ v_1 \end{pmatrix} = T \cdot \begin{pmatrix} f_2 \\ v_2 \end{pmatrix} \tag{2}$$

In use one can directly substitute the T matrix for its circuit symbol. Z can range from a single component to a complicated expression, such as a network of damped tuned circuits, depending upon the requirement.

A library of suitable matrix equivalents for electro-acoustic circuits is shown in Table 2.

For electro-magnetic transducers, the transducer equations $e = Blv$ and $i = f/Bl$ can be expressed in matrix form, as in equation (3).

$$\begin{pmatrix} e \\ i \end{pmatrix} = \begin{pmatrix} 0 & Bl \\ \frac{1}{Bl} & 0 \end{pmatrix} \cdot \begin{pmatrix} f \\ v \end{pmatrix} \tag{3}$$

The form of the T-matrix is that of a gyrator, and an idealized device of this type is lossless, reactance-less, and frequency independent.

More realistic models can be built up with matrix multiplication procedures. For example, a series resistance can be put into the electrical input port by left-multiplying by the appropriate series impedance T-matrix. Similarly mechanical forces due to suspension stiffness, inertia, and so forth can be modelled by right-multiplying the motor's matrix by one describing the motor's mechanical impedance Zm. Finally, if the motor drives a piston of area S, the overall electroacoustic T-matrix for the resulting loudspeaker is shown in equation (4)

$$\begin{pmatrix} e \\ i \end{pmatrix} = \begin{pmatrix} 1 & R \\ 0 & 1 \end{pmatrix} \cdot \begin{pmatrix} 0 & Bl \\ \frac{1}{Bl} & 0 \end{pmatrix} \cdot \begin{pmatrix} 1 & Zm \\ 0 & 1 \end{pmatrix} \cdot \begin{pmatrix} S & 0 \\ 0 & \frac{1}{S} \end{pmatrix} \cdot \begin{pmatrix} p \\ u \end{pmatrix} \tag{4}$$

Equation (4) describes a very idealised loudspeaker, the input being voltage and current, the output being pressure and volume velocity, but more terms are

needed to improve its accuracy. For example voice coils have both resistance and inductance, so the term R in the first T-matrix should be replaced by $R+j\omega L$, and for even more accuracy the R and the L should exhibit the correct dependence on frequency. The mechanical properties of the piston, *Zm* can be expanded upon, ie $Zm = j\omega M + Rs + S/j\omega$.

To incorporate acoustic circuit elements into the T-matrix equation, one formulates the acoustical mesh equations for the input and output pressures and velocities in the form shown in equation (5)

$$\begin{pmatrix} p_1 \\ u_1 \end{pmatrix} = (T).\begin{pmatrix} p_2 \\ u_2 \end{pmatrix} \quad (5)$$

The lumped constant acoustical mass which characterizes a short duct of length *L* and area *S* with a fluid density ρ_0 is shown in equation (6)

$$T = \begin{pmatrix} 1 & \frac{j\omega\rho_0 L}{S} \\ 0 & 1 \end{pmatrix} \quad (6)$$

If a small tube or slit is being modelled then a resistive term needs to be incorporated so that the top right hand matrix term is of the form $R+j\omega L$.

If a small chamber of volume *V* is connected so as to shunt an acoustical flow, the lumped constant acoustical compliance which characterizes the chamber's additional admittance is described by the T-matrix shown in equation (7)

$$T = \begin{pmatrix} 1 & 0 \\ \frac{j\omega V}{\gamma P_0} & 1 \end{pmatrix} \quad (7)$$

Where $\gamma P_0 = \rho_0 c$, ρ_0=density, c=velocity, of sound.

The last matrix building block is a lossless transmission line [8] of area *S* and length *L*, which is described by the T-matrix. ($R_0=\rho_0 c/S$ for acoustic transmission lines) shown in equation (8)

$$T = \begin{pmatrix} \cos(kL) & jR_0 \sin(kL) \\ \frac{j}{R_0}.\sin(kL) & \cos(kL) \end{pmatrix} \quad (8)$$

3.3. SOFTWARE CALCULATION METHOD

The widely available software program, Mathcad, [9] was used. Any mathematical software which can handle matrix algebra with a multi dimensional capacity in that each matrix needs to be calculated for a range of frequencies could be used. The software work sheet was set up in a modular manner so that any changes or additional matrices could be incorporated. Equation (4)

Table 2 T-matrix representation of electrical two-port stages

	Name	***T***	Det ***T***	Zin	Zout	Remarks
	Identity Matrix	1 0 0 1	+1	Z_L	Z_L	
	Series impedance Z	1 Z 0 1	+1	$Z+Z_L$	$Z+Z_L$	
	Shunt Admittance Y	1 0 Y 1	+1	$(Y+Z_L^{-1})^{-1}$		
	Unity gain follower	1 0 0 0	0	∞	0	active
	Operational Amplifier	0 0 0 0	0	indet	indet	active
	Positive Immittance converter (transformer)	n 0 0 1/n	+1	$n^2 Z_L$	Z_L/n^2	Passive if n real
	Negative immittance converter	n 0 0 -1/n	-1	$-n^2 Z_L$	$-Z_L/n^2$	Passive if n imaginary
	Positive immittance inverter (gyrator)	0 Z 1/Z 0	-1	Z^2/Z_L	Z^2/Z_L	Passive if Z real
	Negative immittance inverter (transverter)	0 Z -1/Z 0	+1	$-Z^2/Z_L$	$-Z^2/Z_L$	Passive if Z imaginary
	Transmission line (loss free cylindrical) ($R_0=\rho_0 c/a$ for acoustic)	Cos(kl) jR_0sin(kl) Jsin(kl)/R_0 cos(kl)		R_0	R_0	

could be implemented by first defining each of the matrices representing the various electroacoustic components, and then multiplying them together.

An indexed variable for frequency is created, also for radian frequency ω, shown as ω_j

The first matrix in equation (4), the series impedance representing the frequency dependent voice coil resistance and inductance, is subdivided into two series matrices, as shown in Figure 5.

NOTE: input parameters to yellow fields

Voice coil Re **Voice coil inductance**

$Ree := 5.5$

$Krm := 3.8012\,10^{-5}$ mΩ $Kxm := 1.00\,10^{-3}$ mH

$Erm := 0.9923$ $Exm := 0.774$

$sRee_j := Ree$ $sLe_j := Kxm(\omega_j)^{Exm-1}$

$Rem_j := sRee_j + Krm(\omega_j)^{Erm}$ $Lem_j := j\cdot\omega_j\cdot sLe_j$

$mRe_j := \begin{pmatrix} 1 & Rem_j \\ 0 & 1 \end{pmatrix}$ $mLe_j := \begin{pmatrix} 1 & Lem_j \\ 0 & 1 \end{pmatrix}$

Figure 5 Voice Coil Resistance and Inductance matrices (extract from worksheet)

The static value Ree (Re is reserved for Real Part) is first made into a column vector $sRee_j$, and then the frequency variable part is added. The empirical model for voice coil resistance and inductance uses the parameters Krm, Erm, Kxm, Exm proposed by Wright [10]. The naming convention is fairly obvious; in particular, variables which represent a matrix are prefixed with the letter m.

The next matrix in equation (4), the gyrator, is shown in Figure 6.

Gyrator BL

$BLM := 11.5$

$sBLM_j := BLM$

$mBLM_j := \begin{pmatrix} 0 & sBLM_j \\ \frac{1}{sBLM_j} & 0 \end{pmatrix}$

Figure 6 Gyrator matrix (extract from worksheet)

The next matrix in equation (4) is the moving mass of the diaphragm, modelled as a series mechanical impedance of mass, stiffness, and damping, as shown in Figure 7.

Moving Mass MMD **Compliance CMS** **Mech resistance RMS**

$MMD := 0.003356$ $CMS := 3.39\,10^{-5}$ $RMS := 0.52$

$sMMD_j := j\cdot\omega_j\cdot MMD$ $sCMS_j := \frac{1}{j\cdot\omega_j\cdot CMS}$ $sRMS_j := RMS$

$Zm_j := sMMD_j + sCMS_j + sRMS_j$

$mZm_j := \begin{pmatrix} 1 & Zm_j \\ 0 & 1 \end{pmatrix}$

Figure 7 Mechanical Impedance matrix (extract from worksheet)

In a similar fashion the remaining matrices are created, and can then be multiplied together to obtain a transfer function for the transducer, including any acoustic load.

4. T-MATRIX COMPONENT VALUES

4.1. In-vacuo Measurements

Finding Thiele Small parameters (*M*ms, *R*ms & *C*ms) proved very difficult because of the acoustic loading effects of the structure of the compression driver. A vacuum chamber was used to measure the compression driver's electrical impedance in the absence of air, effectively removing the acoustic matrices in Figure 11. The in-vacuo impedance is plotted in Figure 8, together with a curve obtained by curve fitting and using the Thiele-Small parameters f_s=471.8Hz, *R*e=5.50Ω Q_{ms}=19.1, M_{ms}=3.36gms, C_{ms}=3.39*10^{-5}

The formulae for the voice coil resistance and inductance were developed, curve fitted to the measured impedance data, and the appropriate matrices created for them and the gyrator Bl.

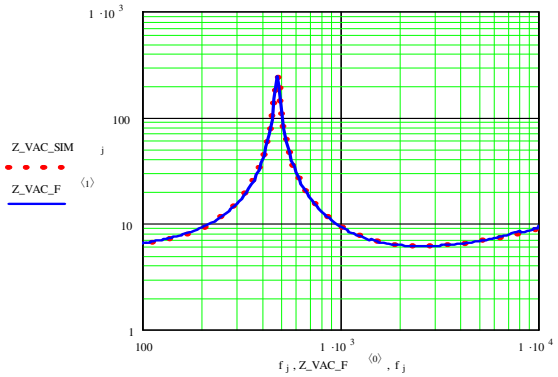

Figure 8 In-vacuo electrical input impedance measured (solid line) versus simulated (broken line)

4.2. Developing Models for Acoustic Losses

The compression driver model loaded with a Plane Wave Tube (PWT) involves all of the matrices described in Figure 11. The resistive damping for the acoustic components was initially calculated on the basis of the formula in Beranek [11] for the acoustic resistance of a slit. His formula 5.51 applies to a rectangular slit, but from an axisymmetric basis the slit was considered to be of a length equal to its circumference, where w is the width (circumference), l is the depth, and t is the thickness (width).

$$Z_A = \frac{12\eta l}{t^3 w} + j\frac{6}{5}\frac{\rho_0 l \omega}{wt} \qquad (9)$$

The first simulation results were problematical, in that the SPL was too high, and the electrical input impedance variations more extreme than that measured experimentally.

Another formula for an annular slit was found in an American Institute of Physics (AIP) text about microphones [12], where the opening is an intermediate-size slot of length (circumference) $2\pi a_k$ width r_k and depth l_k.

$$Z_k = \frac{\sqrt{2\omega\rho_0\mu}}{\pi a_k r_k}\left(1+\frac{l_k}{2r_k}\right) + j\frac{\omega\rho_0 l_k}{2a_k r_k} \qquad (10)$$

This gave significantly different results, as the resistive component increased with frequency, whereas the Beranek model had a resistance constant with frequency. In both the value for the mass of air in the slit was in reasonable agreement. The AIP model seemed more feasible as the principal loss in slits is viscous, and viscous loss increases as the square root of frequency increases. A further refinement for the loss modelling in the voice coil slits was to add a peak in the loss at the fundamental resonant frequency, based on an estimate of the increased loss due to the increased velocity of the diaphragm (and voice coil) excursion at resonance. The simulation results were closer to the experimental, but there are still differences.

The air in the rear enclosure was initially modelled as a simple compliance, and acoustic losses were modelled with both series loss and a parallel leakage loss, nominal values being used initially. Electro-acoustic measurements with the rear cover removed showed changes in the resonance pattern of the SPL and impedance at 2kHz to be more pronounced if the cover was replaced but the fibrous damping was not present. This was clearly a quarter wave stub effect inside the rear enclosure, quite pronounced because of the circular nature of the diaphragm and the enclosure. It was approximated as a simple series resonant circuit at the fundamental frequency. The rear enclosure should strictly be modelled connected between the negative terminal of the output of the $1:{}^{1}/_{SD}$ transformer and ground, but the overall effect seemed to be the same if its impedance was connected in series with the positive terminal and the remainder of the acoustic circuit.

The air immediately under the diaphragm was modeled as a small mass and resistance and compliance, as proposed by Henricksen [13]. He argued that there was a 'stagnant point' of air along the half way line between the slits under the diaphragm. He took into account this small path length from the 'stagnant point' to the slits themselves, as a series mass and resistance before the small volume of air under the diaphragm.

The air under the diaphragm has two exit paths, one through the slits to the outside, the other past the voice coil and into the interior. This path was modelled as a series of annular slits and annular volumes, developing into a surprisingly complex equivalent circuit. A discrepancy in SPL and impedance at 400Hz could only be reproduced by the inclusion of an internal Helmholtz resonator, and the most likely possibility was further leakage paths past each end of an aluminium flat ring into the magnet cavity. When this was modelled and a suitably small value assigned to the clearance slit past the flat aluminium ring, the SPL and impedance graphs assumed their correct form, and it only remained to adjust the circuit values by adjusting the width of the leakage slits to achieve a suitable value of damping. The lengths of the slits were obtained from physical measurements, but the widths could only be estimated.

The phase plug and the path through the compression driver to the outside were modeled as transmission line segments; dimensions such as starting cross sectional area, finishing area, and length, being derived from physical measurements. The appropriate values for the entries into the formulae in a matrix were calculated. The acoustic resistance of the fine metal mesh between the last two segments was also calculated, and modelled as a matrix for a small series resistance.

The easiest part was developing a model for the plane wave tube – a simple resistor of value ρ_0/S as a parallel element as the last matrix.

As mentioned above, experimental SPL measurements were made of the compression driver with the back removed, and with the back present but no fibrous damping. These proved useful in isolating the plurality of resonances in the low kHz frequency band.

5. TRANSMISSION MATRIX MODELLING

The geometry of the compression driver can be redrawn to clarify the acoustic circuit and is shown in Figure 9.

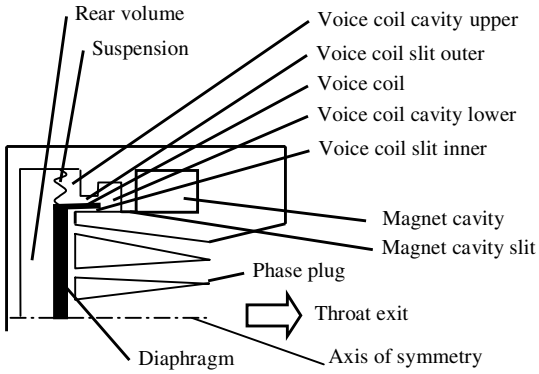

Figure 9 Simplified geometry of compression driver

It can be seen that movement of the diaphragm to the right compresses the air between it and the phase plugs, and air flows through the phase plugs to the exit. Movement of the diaphragm also forces air to flow down between the voice coil and the pole piece through the slit passage labeled “voice coil slit inner” and into the cavity labelled “voice coil cavity lower”. From there the flow divides, part going through the slit passage labeled “voice coil slit outer” and into the cavity labelled “voice coil cavity upper’. The remaining flow passes through the slit passages labelled “magnet cavity slit inner” and “magnet cavity slit outer” into the cavity labelled “magnet cavity”.

The air flow through the phase plugs to the outside is essentially a group of transmission lines in parallel, each of nominally the same length. The air flow encounters a mesh screen, usually fitted to minimise the ingress of foreign objects. There is a further leakage slit into the volume of the aluminium casting on the front of the compression driver. The remaining distance to the throat exit can be modeled as a short transmission line.

The equivalent circuit shown in Figure 10 can be converted to a T-matrix representation using techniques described in a previous section. The cascade of matrices is shown in Figure 11. Note that the matrices in bold represent transduction between domains.

5.1. Transmission Matrix Results

Figure 12, 13 and 14 show the T-matrix simulated results compared to experimental measurements.

The SPL shows good overall agreement, the difference being of the order of a dB over the operating range of frequencies. The measured 450Hz dip is a result of air leakage into the magnet cavity, and the T-matrix had to be extended to be able to model it. There is another notch at about 85Hz, which was traced to leakage into the volume behind the aluminium front casting. The notch at about 2.5kHz is due to a standing wave in the rear cavity, as it is much worse when there is no fibrous absorption in the rear cover, and disappears when the compression driver is measured with no rear cover.

The electrical impedance magnitude shows good agreement, especially when the 450Hz dip is modeled. The measured impedance peak shows a subtle change of slope in the 300-400Hz region, which is due to the notch. It shows more clearly on the impedance phase curve, and only a Helmholtz resonator *across* the internal pressure gives the correct shape to both the SPL and the electrical impedance.

The rear volume standing wave is modelled as a simple tuned circuit at 2.5kHz across the internal pressure. While the SPL shows the appropriate notch, the electrical impedance curve shapes are not quite correct. As mentioned previously, this effect should be modelled by a lossy quarter wave stub, and the rear impedance itself is modelled as a compliance in series with the positive output terminal of the source S_D, rather than being connected between the negative terminal and ground, thereby making the whole T-matrix model a parallel configuration, and much more complicated to evaluate using Lampton’s methods.

The equivalent circuit and matrix are shown in Figures 10 and 11

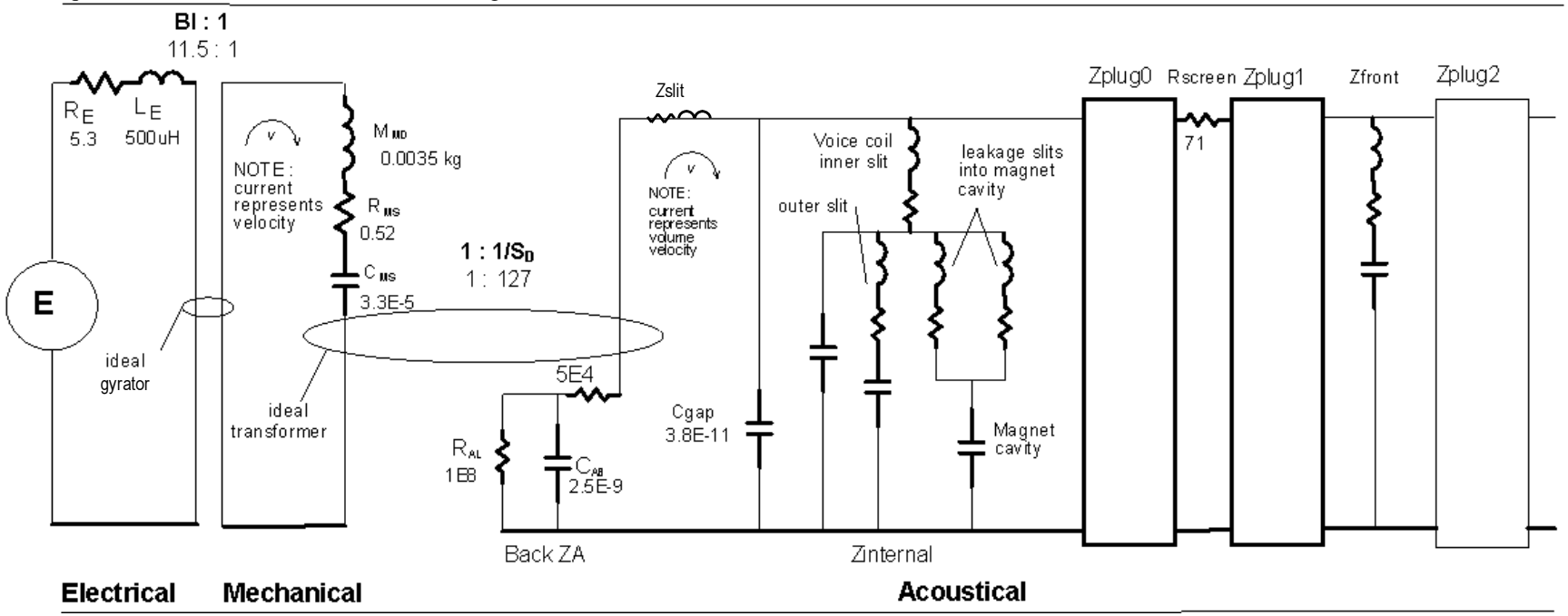

Figure 10 Electrical, Acoustical, and Mechanical equivalent circuit of a compression driver.

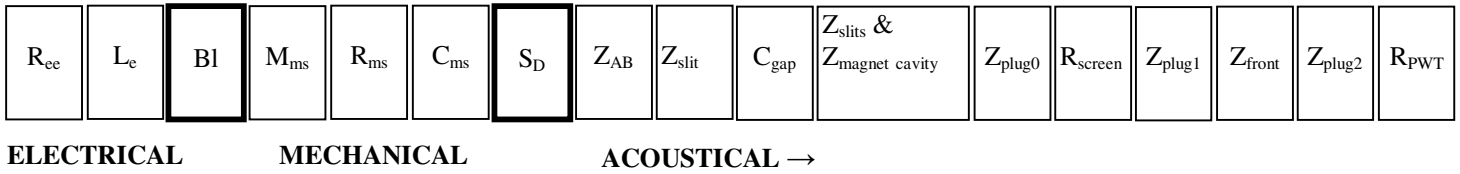

Figure 11 T-matrix representation of a compression driver. The matrices in bold represent transduction between domains.

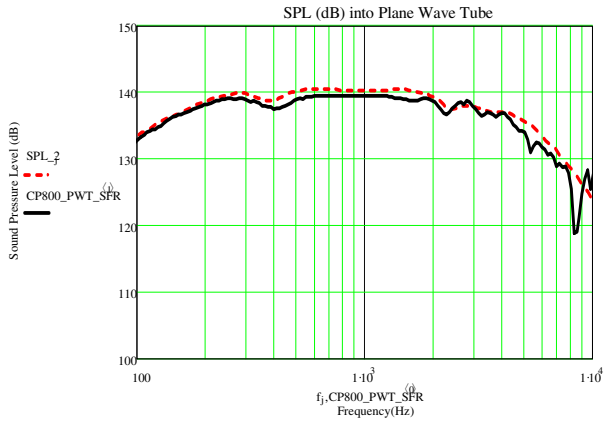

Figure 12 Measured (solid line) versus T-matrix simulated (broken line) SPL into a Plane Wave Tube (resistive load)

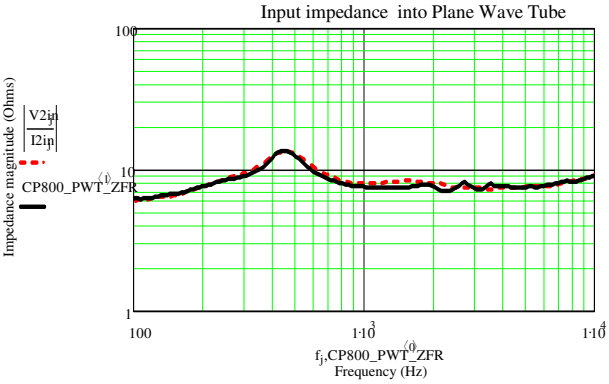

Figure 13 Measured (solid line) versus T-matrix simulated (broken line) electrical input impedance magnitude

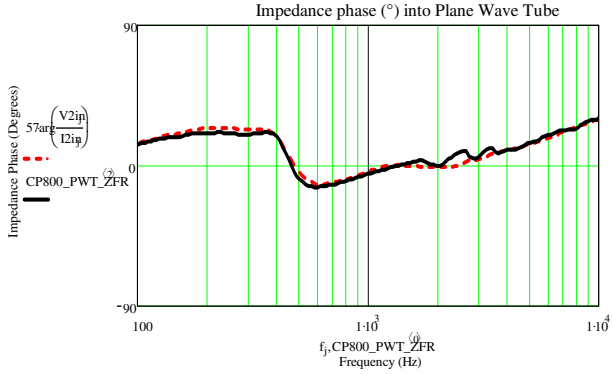

Figure 14 Measured (solid line) versus T-matrix simulated (broken line) electrical input impedance phase

6. FINITE ELEMENT ANALYSIS METHOD

The finite element technique [14], or Finite Element Analysis (FEA) is a general numerical method that can be used to solve a partial differential equation with appropriate boundary conditions. It has been used to solve problems in a wide variety of areas such as heat transfer, linear and non-linear solid mechanics, and fluid flow.

In acoustical fluid-structure interaction problems, the structural dynamics equation needs to be considered along with the equations of fluid momentum and the flow continuity equation. The discretised structural dynamics equation can be formulated using structural elements, and the fluid equations are simplified to get the acoustic wave equation using the following assumptions:

- The fluid is compressible (density changes due to pressure variations)
- The fluid is inviscid (no viscous dissipation)
- There is no mean flow of the fluid
- The mean density and pressure are uniform throughout the fluid.

The acoustic wave equation is given by:

$$\frac{1}{c^2}\frac{\partial^2 P}{\partial t^2} - \nabla^2 P = 0 \qquad (8)$$

where c = speed of sound $\left(\sqrt{k/\rho_0}\right)$, ρ_0 = mean fluid density, k = bulk modulus of fluid, P = acoustic pressure (P(x,y,z,t), and t = time.

For harmonically varying pressure, ie $p=P\,e^{j\omega t}$ where $\overline{P}$ is the amplitude of the pressure, $j=\sqrt{-1}$, $\omega=2\pi f$, f=frequency of oscillations of the pressure, the equation (8) reduces to the Helmholtz equation.

$$\frac{\omega^2}{c^2}\overline{P} + \nabla^2 \overline{P} = 0 \qquad (9)$$

FEA involves discretising or "breaking up" a domain of interest into smaller "finite" elements, and the underlying differential equation is approximated over these elements. This leads to a system of linear equations which are solved after the application of boundary conditions to provide a solution for the whole domain.

For these techniques to give accurate results for acoustic problems, the elements need to be a small fraction of an acoustic wavelength in size, $^1/_6$ of a wavelength being recommended. As the frequency considered in the analysis increases, the acoustic wavelength decreases, and the corresponding number of elements required to accurately model a component of a given physical size increases approximately as the cube of frequency, with a corresponding increase in computational time and memory requirements.

Using FEA with modern commercial software packages is straight forward: a three dimensional model of the geometry is developed or imported, the geometry is meshed, boundary conditions are applied, the problem is solved, and the data is analysed. The input parameter is a force or acceleration or flow, and the outputs are real and imaginary parts of pressure or velocity for each element. To gain confidence in the FEA results, the results of text book acoustic examples (piston in infinite baffle) were developed and verified.

In practice, obtaining a good mesh is not easy! Earlier versions of the FEA software were certified only for quadrilateral elements for acoustics, and some ingenuity was needed in meshing. Tetrahedral elements were able to be used in later versions of the FEA software, which made the meshing process much easier.

To obtain results easily comparable to experimental measurements the electrical input voltage needed to back calculated through electro-mechanical force conversion, and the dB SPL calculated from the real and imaginary parts of the pressure averaged over the elements comprising the throat exit.

7. FINITE ELEMENT MODELLING

The Finite Element Analysis (FEA) method, requires no such assumptions, and models can be easily constructed based on the measured physical geometry.

A quarter symmetric finite element mesh was constructed using the ANSYS commercial FEA package. Figure 15 and 16 show the mesh used. Care was needed to obtain elements of good shape and to ensure adequate density with smooth variation of the density of the mesh at the highest operating frequency. The element size used was calculated for the highest anticipated simulation frequency, although of necessity some small spaces were meshed more finely.

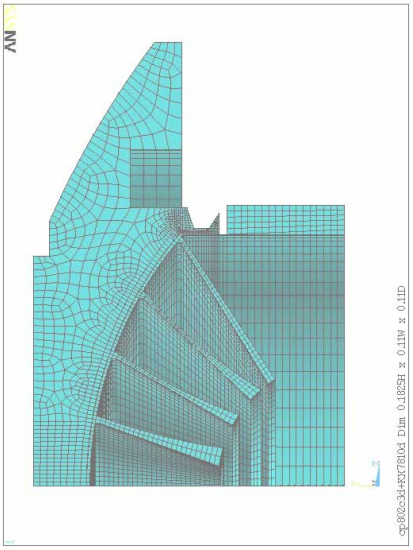

Figure 15 Finite element mesh of air inside the compression driver. Remainder of phase plugs and front air in PWT created and meshed separately for each frequency.

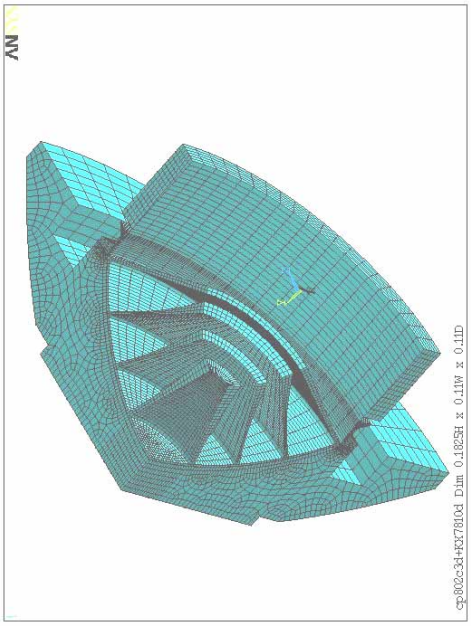

Figure 16 Perspective view of finite element mesh of compression driver

To ameliorate the size of the problem increasing too much at high frequencies, and the subsequent increase in time of the simulation, most of the compression driver was meshed for 20kHz, and the remainder of the air of the compression driver and PWT was meshed appropriately for the frequency of the simulation. To obtain the least amount of standing waves in the PWT it was found that the length needed to be slightly more than half a wave length.

A crucial feature of the FEA program was its Advanced Programming and Development Language (APDL), enabling a complex suite of macros and subroutines to be written. These calculated an array of frequencies, imported the meshed compression driver, created a PWT structure mated to the front of it, meshed the PWT, selected groups of elements and named them for later extraction of results, applied boundary conditions such as x, y, z constraints, absorption surfaces, and applied a force/acceleration /flow as the input stimulus. Then the problem was solved, and the raw pressure/velocity results were extracted for each element. The SPL in the PWT was computed by averaging the pressure of a small number of elements on the side wall where the microphone was located on the physical PWT.

The force applied to the diaphragm was known, the velocity/displacement was extracted from the diaphragm elements and averaged, and the mechanical impedance calculated. This could be used in a back calculation through the S_D transformer and the Bl gyrator to an equivalent electrical impedance, and the electrical input voltage calculated. This was then scaled to 2.83 volts, and forward calculated to give a scaled SPL. These results were stored for each frequency.

The first complete debugged run gave curious results, the SPL was a couple of dB too high, and variations in SPL and electrical input impedance were exaggerated. It was quickly realized that there was appreciable absorption of energy inside the compression driver, mostly due to viscous losses because of the confined acoustic spaces inside the compression driver.

A considerable amount of development work was needed to isolate and apply appropriate damping. Apart from global application, the only available damping in the FEA program was applying absorption to specific surfaces, so the solution was to develop more macros to apply frequency dependent absorption to simulate the action of the frequency (velocity) dependent losses. Absorption that was constant with frequency didn't close the gap between simulated and measured results, nor did a simple increase as the square root of frequency model. The closest match to date has been obtained with absorption rising as the square root of frequency, with additional increases at relevant frequencies for the spaces involved. For example, the voice coil annular slits had absorption applied which rose as the square root of frequency rose and incorporated an extra 'graphic equalizer' increase at the fundamental resonant frequency based on the estimated Q factor of that resonance. The phase plug slits had a similar increase of absorption based on the square root of frequency and extra absorption based on the estimated Q factor of the variation of SPL at those frequencies.

This methodology enabled quite close matching of the SPL response (Figure 17), although the electrical input impedance results (Figure 18) are not as close. Compared to the T-matrix the SPL is closer, but the electrical input impedance magnitude and phase diverge. The FEA model is able to achieve more damping in the front spaces of the compression driver because absorption is applied to all the phase plug areas under the diaphragm, and the slits in the phase plug, and the voice coil slits. Unfortunately this is necessary but not sufficient, as it achieves an SPL match but not an impedance match to measured results.

There is a resonance in the SPL response at 6kHz which is undamped in the ANSYS simulation, but damped in the measured, and a further SPL resonance at 9kHz where simulated and measured go in opposite directions! This last frequency is where in real life the titanium diaphragm is losing its piston action. This is not simulated correctly when the air under the diaphragm has a uniform force applied to it, rather than a full Fluid Structure Interaction simulation.

7.1. Finite Element Analysis Results

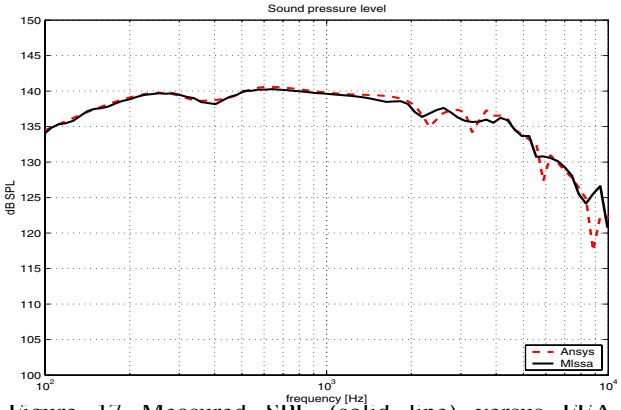

Figure 17 Measured SPL (solid line) versus FEA simulated (broken line)

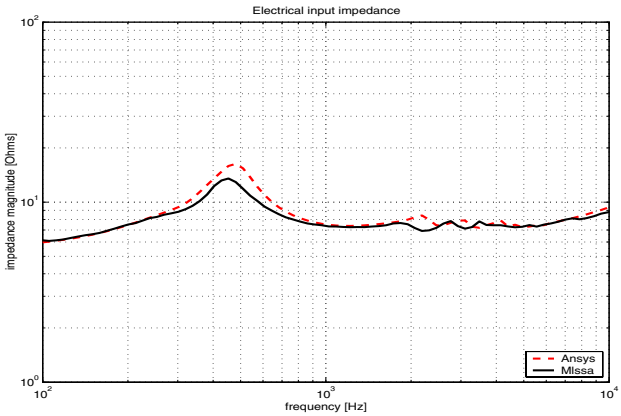

Figure 18 Measured electrical input impedance magnitude (solid line) versus FEA simulated (broken line)

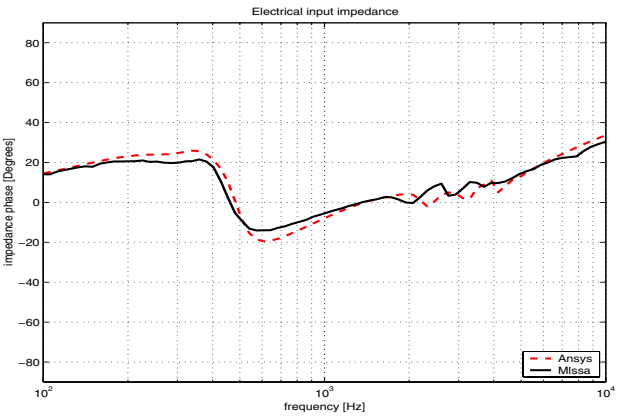

Figure 19 Measured electrical input impedance phase (solid line) versus FEA simulated (broken line)

8. CONCLUSIONS

The T-matrix method showed itself capable of modelling the compression driver to a level of accuracy suitable for design of high performance audio equipment. However, the modelling of the acoustic elements required significant physical insight and experience in order to achieve the desired performance. It required accurate estimation of the path lengths and cavity volumes in the compression driver. It required the development of sophisticated models of acoustic damping. The T-matrix approach is limited in its ability at high frequencies.

An alternative modelling approach, the Finite Element Analysis (FEA) method, required no such assumptions, and models can be easily constructed based on the measured physical geometry. A quarter symmetric finite element mesh was constructed using the ANSYS commercial FEA package, effectively modelling all acoustic loading paths. It assumed an infinitely stiff diaphragm and provided significant savings in computational time over other approaches that couple the mechanical to the acoustic domain. It required the development of sophisticated models of acoustic damping.

The electrical impedance of the compression driver was measured in a vacuum chamber to isolate the effects of the acoustic loading and thus obtain the basic Thiele-Small parameters of the titanium diaphragm.

For both approaches another compression driver was cut in half to investigate its physical layout and verify the manufacturer's engineering drawing. A 450Hz resonance that was seen experimentally could only be modeled by assuming a Helmholtz resonator (damped series resonance) across the output, and the most likely cause was a leakage path into the magnet cavity. This change was incorporated into both models.

Both models were able to calculate electrical input impedance and sound pressure levels in the plane wave tube, and these results were compared to experimental measurements. It was found that there was a significant damping effect in the small spaces of the compression driver. In order to accurately match the measured SPL and electrical impedance, it was found that frequency dependent damping was required in both models.

9. ACKNOWLEDGEMENTS

This work was supported by **Krix Loudspeakers**, 14 Chapman Road HACKHAM AU5163 South Australia.

10. REFERENCES

[1] W. M. Leach, *On the specification of moving-coil drivers for low-frequency horn-loaded loudspeakers*, JAES **27**(12) 950-959, (1979)
[2] Geddes, E. Clark, D. *Computer Simulation of Horn-Loaded Compression Drivers*, JAES Volume **35** (7/8) 556-566, (1987)
[3] Beltran, C. I., *Calculated Response of a Compression Driver Using a Coupled Field Finite Element Analysis*, Preprint 4787; AES Convention 105; (1998)
[4] JBL Technical Notes Volume 1 , Number 8 (date unknown)
[5] Acustica Beyma, Pol. Ind. Moncada II, Carrer del Pont Sec, 1c 46113 MONCADA VALENCIA ESPANA www.beyma.com
[6] Bauer, B. B. *Equivalent Circuit Analysis of Mechano-Acoustic Structures* JAES Volume **24** (10) pp643-652 (1976 October)
[7] Lampton, M. *Transmission Matrices in Electroacoustics* ACUSTICA Volume 39 239-251 (1978)
[8] Mapes-Riordan, D. *Horn Modelling with conical and cylindrical transmission-line elements* JAES Volume **41**:6 pp471-484 (1993 June)
[9] Mathcad 6 to Mathcad 2000, by MathSoft Inc Cambridge MA USA www.mathsoft.com
[10] Wright, J.R. *An Empirical method for loudspeaker motor impedance* JAES Volume 38(10) 749-754, (1990)
[11] Beranek Leo. L. *Acoustics* published by the Acoustical Society of America through the American Institute of Physics 1993
[12] Zuckerwar, Allan J. *Physical Principles of Condenser Microphones* Chap 3 AIP Handbook of Condenser Microphones American Institute of Physics (1995)
[13] Henricksen, Clifford A. *Phase Plug Modelling and Analysis: Radial versus Circumferential Types* AES Preprint 1328 59th Convention, (Feb28-Mar 3 1978)
[14] Kohnke, P. editor. *ANSYS 5.5 Theory Manual*. Ninth Edition, 1998 Ansys Inc, Southpointe 275 Technology drive, Canonsburg, PA, 15317 www.ansys.com